Transport Properties of Polypyrrole Films Doped with Sulphonic Acids

C. Basavaraja, Na Ri Kim, Eun Ae Jo, R. Pierson, Do Sung Huh,* and A. Venkataraman†

Department of Chemistry and Institute of Basic Sicence, Inje University, Kimhae, Kyungnam 621-749, Korea
**E-mail: chemhds@inje.ac.kr*
†Department of Materials Science, Gulbarga University, Gulbarga, Karnataka, India
Received August 2, 2009, Accepted September 30, 2009

The polymer blends containing polypyrrole (PPy) and the sulphonic acids such as β-naphthalene sulfonic acid (NSA), camphor sulfonic acid (CSA), and dodecylbenzenesulfonic acid (DBSA) were synthesized by *in situ* deposition technique in an aqueous media using ammonium per sulfate (APS) as an initiator. The obtained films were characterized by scanning electron microscopy (SEM), and the thermal behavior of these polymer blends was analyzed by thermogravimetric analysis (TGA) and differential scanning calorimetry (DSC). The temperature-dependent (DC) conductivity of the obtained films shows a semiconducting behavior with a negative temperature coefficient of resistivity (TCR). The conductivity data were also analyzed through Mott's equation, which provides the variable range hopping model in three dimensions. The parameters such as density of states at the Fermi energy, hopping energy, and hopping distance were calculated for PPy, PPy-NSA, PPy-CSA, and PPy-DBSA films, and the data were compared.

Key Words: Mott's equation, Polypyrrole, Sulphonic acids

Introduction

In recent years, intrinsic conducting polymers (CPs) with conjugated double bonds have attracted much attention as advanced materials. Among the CPs, polypyrrole (PPy) is especially promising in commercial applications because of its good environmental stability, facile synthesis, and higher conductivity compared with many other conducting polymers. PPy can often be used as biosensors,[1,2] gas sensors,[3,4] wires,[5] microactuators,[6] antielectrostatic coatings,[7] solid electrolytic capacitor,[8] electrochromic windows, displays, and packaging, polymeric batteries, electronic devices and functional membranes, and so on.[9,10] PPy coatings have an excellent thermal stability and are good candidates for use in carbon composites.[11] Furthermore, the electrochemical process parameters affecting the properties of the PPy coatings are also investigated.[12] PPy can be easily prepared by either an oxidative chemical or electrochemical polymerization of pyrrole and doped by a simple operation. However, synthetically conductive PPy is insoluble and infusible, which restricts its processing and applications in other fields. The problem has been extensively investigated and new application fields have also been explored in the past several years. It is well-known that electric and mechanical properties depend on the synthesis conditions, substrate, electropolymerization potential or current density, and in particular, the nature and concentration of the synthesis solutions.

In recent years, the template method has been introduced to improve the infusibility and processability of the CPs. In the template method, the target material is precipitated or polymerized on the surface of the template, which results in a core-shell structure. By removing the template, hollow microspheres can be obtained. However the removal of the template often affects the spherical structure, especially for hollow polymer microspheres. Most recently, hard templates have been used in carbon nanotubes,[13] lipid tubule edges,[14] and electrospun polymer fibers[15] for synthesizing micrometer-/nanometer-sized conducting polymers. However, to obtain appropriate hard-template materials, scientists have to purchase or prepare appropriate porous materials before synthesizing the prospective materials. Moreover, to get pure conducting polymers, the hard-template materials have to be removed after synthesis. This is very difficult in most cases and may drastically alter or even destroy the resulting materials during recovery from the templates. However, soft-templates or molecule templates are often long-range ordered structures self-assembled from certain surfactants or block copolymers and others, which provide well-defined rooms or channels for conducting polymer chains to grow into micrometer-/nanometer-sized products.[16,17] The advantage of using these soft-template materials is that they are easy to remove after synthesis, allowing the micro-/nanostructures of the resulting polymers to remain.

On the other hand, the emulsion template method can be a good candidate since the emulsion can be easily removed through dissolution or evaporation after polymerization. In fact, the essence of the emulsion template process is the self assembly of the target materials on the surface of the emulsion droplets through polymerization or deposition. Replacing mineral acid dopants such as HCl or H_2SO_4 with functionalized organic acids such as camphorsulfonic acid (CSA) and 2-acrylamido-2-methyl-1-propanesulfonic acid (AMPSA)[18] increases the overall solubility by way of the large organic groups attached to the acidic moiety. Other sulfonic acids are effective as dopants, including polyelectrolytes such as polystyrenesulfonic acid,[19-21] diesters of sulfophthallic acid,[22] and sulfosuccinic acid,[23] particularly in association with polar solvents such as *m*-cresol or 2,2-dichloroacetic acid (DCAA).

In the present study, the PPy films were synthesized by *in situ* deposition technique using pyrrole and different emulsifying surfactants such as NSA, CSA, and DBSA with APS as an initiator. These films were characterized for morphology and thermal stability using SEM, TGA, and DSC. The temperature-dependent DC conductivity of the obtained composites was studied,

and further TCR values and activation energy were obtained. The conductivity data were also analyzed through Mott's equation, which provides the variable range hopping model in three dimensions. The parameters such as density of states at the Fermi energy, hopping energy, and hopping distance were calculated for PPy, PPy-NSA, PPy-CSA, and PPy-DBSA films, and the data were compared.

Experimental

Materials. All the chemicals used for the synthesis of PPy and its composites were purchased from Sigma-Aldrich and were utilized without further purification. *N*-methyl-2-pyrrolidinone (NMP) was obtained from Junsei Chemical Co.

Synthesis of PPy and PPy-sulphonic acid blends. The polypyrrole-sulphonic acid blends were synthesized by *in situ* doping polymerization in the presence of sulphonic acid as the dopant without an external template. This method belongs to the self-assembly process because the dopant serves both the doping and template functions at the same time. A typical preparation process of these nanocomposites proceeded as follows: the sulphonic acids along with the pyrrole monomer were first dissolved in water, and the solution was kept under ultrasonication for 2 h to obtain a uniform suspension containing pyrrole-surfactant. The APS solution was then added slowly, followed by cooling to −10 °C of the complete solution. The resulting mixture was allowed to react in an ice bath for 20 h. The precipitated powder was filtered and washed with distilled water and methanol until the filtrate became colorless, and was then dried in a vacuum at room temperature for 24 h. To compare the effects of the surfactant on the morphologies of the resulting PPy nanostructures, the molar concentration of pyrrole and the sulphonic acids NSA, DBSA, and CSA were kept constant at 0.05 M. The blends were abbreviated as PPy for without surfactant, and PPy-NSA, PPy-CSA, and PPy-DBSA for with sulphonic acids of NSA, CSA, and DBSA, respectively.

Afterwards, the resulting precipitate was filtered and washed thoroughly with deionized water and acetone. It was dried under vacuum for 24 h to achieve constant weight. The powder was treated with a solution of sodium ethoxide (C_2H_5ONa) and ethanol, and was magnetically stirred at room temperature for 12 h. Finally, the precipitate was filtered and washed repeatedly with ethanol and stored in a desiccator for 4 h at room temperature. About 2 g of obtained powder was taken in 30 mL of NMP solution, magnetically stirred for 24 h at room temperature. The solution was then placed on a Petri dish, and the NMP solvent was allowed to evaporate at 45 °C for 48 h. The obtained films were then placed in distilled water, rinsed with ethanol, and dried at room temperature for another 24 h. To obtain solvent-free films, the residual NMP was removed by three cycles of doping using 1 M HCl solution for 18 h and de-doped by 0.1 M NH_4OH solution for another 18 h at room temperature. The resulting NMP-free composite films were cleaned in deionized water and dried at room temperature for about one day.[24]

Characterization and property evaluation of the composites. The morphology of the synthesized composite films was investigated by using SEM (Philips XL-30 ESEM). The samples for SEM were mounted on aluminum studs using an adhesive graphite tape and were sputter-coated with gold before analysis. Thermal properties were obtained by TGA (Perkin Elmer model TGA 7) and DSC by (Perkin Elmer model DSC 7) in the range 20 to 800 °C at 2 °C/min in nitrogen atmosphere. The DC electric measurements of the obtained composite films were performed within the temperature range of 300 to 500 K using the four-probe technique with a Keithly 224 constant current source and a Keithly 617 digital electrometer.

Results and Discussion

Polymerization mechanism. PPy forms complexes with sulfonic acids. When the acid molecule is amphiliphilic, the polymer backbone can become complexes with the NSA, DBSA, or CSA molecules, and the complex forms are reported to form lamellar self-organized structures with alternating polar and nonpolar layers.[21-23] The complexation of PPy with sulfonic acids is regarded to be through hydrogen bonding between the sulfonic acid and the nitrogen of PPy, while the protonation is considered to occur in the nitrogen atom of PPy.[22,23] The pyrrole monomers are encapsulated into uniform spherical micelles or between periodical lamellar structures driven by the hydrophobic interaction. There may be a saturated monomer concentration at which the micelles can accommodate the maximum number of monomers because the total interior volume of micelles or lamellae is definite at an equilibrium state once the surfactant concentration remains fixed.[22,23]

Morphology. Figs. 1(a), (b), and (c) show the FESEM images

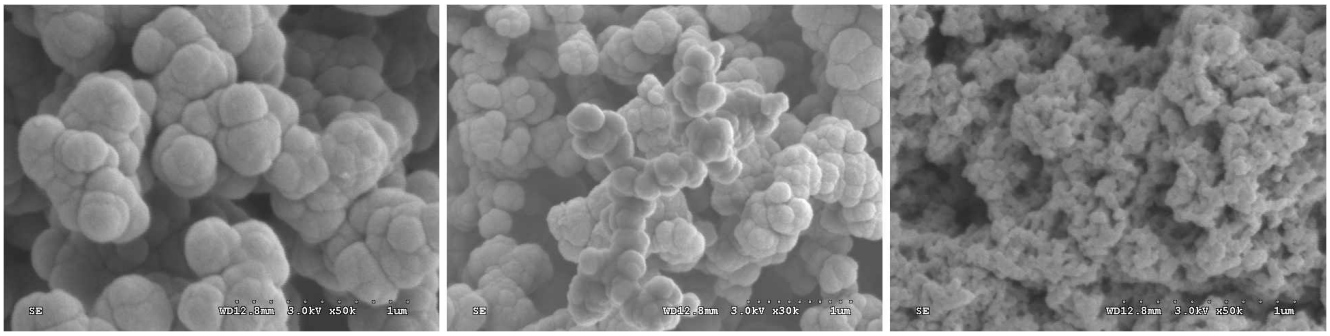

(a) (b) (c)

Figure 1. SEM images showing the morphology of PPy-NSA (a), PPy- CSA (b), and PPy-DBSA (c).

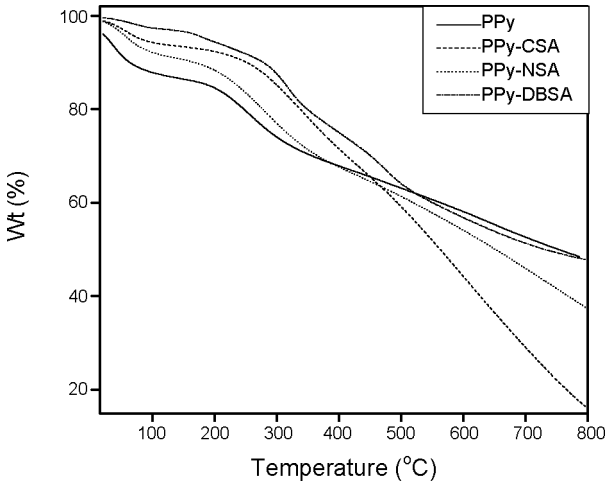

Figure 2. TGA curves of PPy, PPy-NSA, PPy-CSA, and PPy-DBSA.

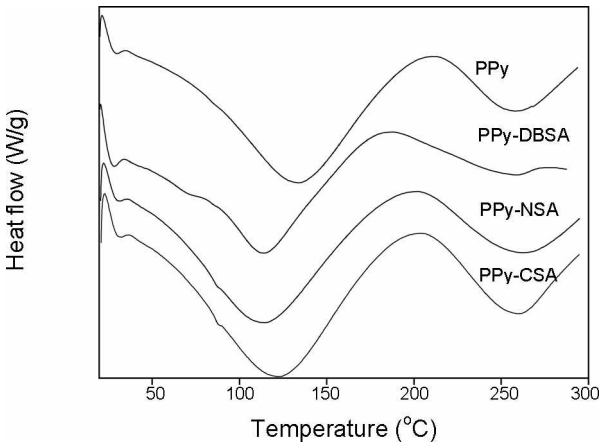

Figure 3. DSC curves of PPy, PPy-NSA, PPy-CSA, and PPy-DBSA.

of PPy-NSA, PPy-CSA, and PPy-DBSA, respectively. We can see clearly from the figures that the morphology of PPy is influenced greatly depending on the presence of different sulphonic acid units. In Fig. 1(a), the surface structure of PPy-NSA particles is shown at a magnification of 50 K. The PPy-NSA particles appear to be spherical, while the surface forms a cauliflower-like morphology. The size of these particles lies in the range of 270 nm to 330 nm. Fig. 1(b) represents the surface structure of the PPy-CSA composite particles, which are shown at a magnification of 30 K. The surface indicates a one-dimensional nanostructure with spherical nanoparticles, and the particle size of the PPy-CSA ranges from 230 ~ 260 nm. Fig. 1(c) indicates the surface structure of PPy-DBSA, which is shown at a magnification of 50 K. The morphology is a phase-segregated type which reveals a "broken eggshell-like" morphology, and the particle size of this composite ranges between 60 ~ 75 nm.

After observing the SEM images of the composites it appears as that the pyrrole monomer units are first dispersed in aqueous solutions under different sulfonic acid environment by NSA, CSA and DBSA to form different micelles. The structure of these micelles remains same inducing different composite structures as obtained by the SEM images as shown in Figs. 1. Thus the structure of the sulfonic acids plays a major role in the composition of the composites.

Table 1. Comparison of the degradation behavior of PPy, PPy-CSA, PPy-NSA, and PPy-DBSA at different temperatures.

Composite	Weight loss (wt%) at different temperatures (°C)			
	300	400	500	800
PPy	74	67	63	47
PPy-CSA	85	71	59	16
PPy-NSA	77	67	61	37
PPy-DBSA	87	75	64	46

Thermal studies. Fig. 2 shows the TGA curves for PPy, PPy-NSA, PPy-CSA, and PPy-DBSA. The PPy and PPy-sulphonic acid follow three steps during the decomposition processes. The initial stages of weight loss are due to the volatilization of water molecules and oligomers, as well as unreacted monomer elimination. At higher temperatures, the protonic acid component of the polymer is then lost, and finally, at more extreme temperatures, the break of the polymer chain can lead to the production of volatile gases. PPy-sulphonic acids are thermally stable in the range of 10 to 400 °C. Beyond this temperature range, the decomposition process becomes very rapid. PPy is somewhat more stable thermally than the PPy-sulphonic acids. This may be due to the higher weight losses before the thermal breakdown of the polymer backbone in the blends. The comparison between the degradation behavior of the PPy and those of PPy-NSA, PPy-CSA, and PPy-DBSA composites is summarized in Table 1. For PPy, the TGA curve shows that the decomposition begins at around 300 °C, while for PPy-CSA, PPy-NSA, and PPy-DBSA, the decomposition temperature is formed at around 300 to 400 °C after water loss.

Fig. 3 shows the DSC curves for PPy, PPy-NSA, PPy-CSA, and PPy-DBSA. DSC curves for the same forms of PPy show the first endothermic peak at around 134 °C, which may be the glass transition temperature (T_g) for PPy. For PPy-CSA, PPy-NSA, and PPy-DBSA, the values of T_g are around 120 °C, 115 °C, and 116 °C, respectively. The second endothermic peak for PPy is at around 258 °C, and for PPy-CSA, PPy-NSA, and PPy-DBSA composites, it is at 259 °C, 262 °C, and 264 °C, respectively. The variation in the endothermic peaks for the composites may be due to the presence of different sulphonic acids present in the composite samples. There is a shoulder present both in PPy and PPy-CSA, which is less in PPy-NSA and PPy-DBSA, indicating the less orderness of the polymer PPy and PPy-CSA than PPy-NSA and PPy-DBSA. The increase in the glass transition temperature in the PPy-CSA, PPy-NSA, and PPy-DBSA is due to the attainment of the longer chain length. The increase in chain length may be due to the presence of sulphonic acid along with the polymer PPy.

Electrical properties of the of PPy and PPy-sulphonic acid films. Fig. 4 indicates the variation of electrical resistivity (Ω) with temperature for PPy-surlphonic acid composites obtained between the temperatures 300 K and 500 K. The values Ω decrease exponentially with temperature similar with a semiconducting behavior, and they basically depend on the type of sulphonic acid used. The value of Ω is higher at a low temperature and decreases as the temperature increases. The temperature coefficient of resistivity (TCR) for PPy, PPy-NSA, PPy-CSA, and

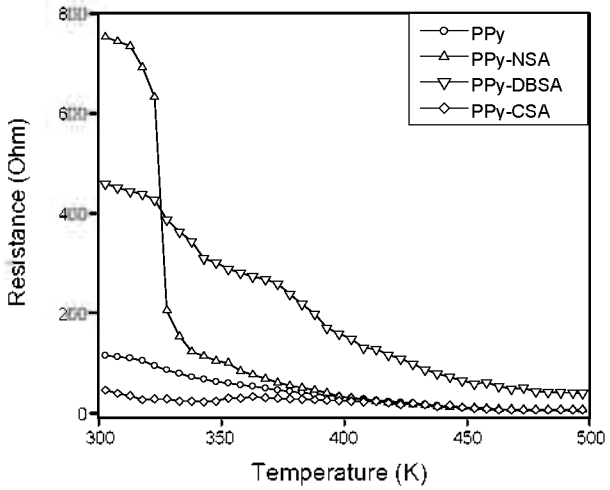

Figure 4. Temperature dependence of electrical resistance for PPy, PPy-NSA, PPy-CSA, and PPy-DBSA.

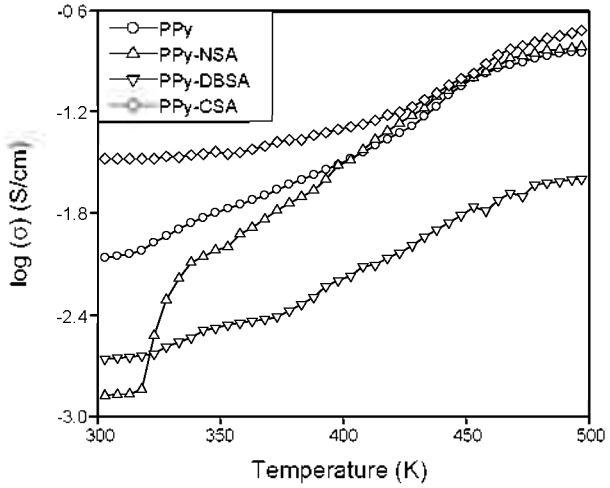

Figure 5. Temperature dependence of conductivity in logarithm for PPy, PPy-NSA, PPy-CSA, and PPy-DBSA.

PPy-DBSA were determined from the variation of electrical resistivity with temperature using the following relation:[25]

$$\mathrm{TCR} = \left(\frac{1}{\rho(T_1)}\right)\left(\frac{\Delta\rho}{\Delta T}\right) \quad (1)$$

where $\Delta\rho = \rho(T_1) - \rho(T_2)$, and $\Delta T = T_2 - T_1$. Table 2 presents the calculated TCR values for PPy and PPy-sulphonic acids at different temperature ranges, which show that they have negative values and remain unchanged with temperature. Table 2 indicates that the TCR values increase as the temperature increases except for PPy-NSA, in which the TCR values decrease with the increase in temperature. The conducting polymers are typically aligned in the form of chains interspersed with regions where the chains are disordered.[26-29] and it is assumed that there are highly conducting islands in a sea of amorphous polymer. The suphonic acids such as NSA, CSA, and DBSA have a positive influence on the temperature-dependent conducting property of PPy, which is caused by the mobility of counterions of the surfactants at higher temperature.

Table 2. Calculated values of the temperature coefficient of resistivity (TCR) for PPy, PPy-CSA, PPy-NSA, and PPy-DBSA at different temperature ranges.

Temperature (K)	Temperature coefficient of resistivity (TCR)			
	PPy	PPy-NSA	PPy-CSA	PPy-DBSA
300 ~ 350	-0.00971	-0.0173	-0.00683	-0.00743
350 ~ 400	-0.00985	-0.0139	-0.00955	-0.00972
400 ~ 450	-0.0143	-0.0130	-0.01200	-0.01220
450 ~ 500	-0.0146	-0.0102	-0.01230	-0.01240

Table 3. Calculated values of E_σ for PPy, PPy-CSA, PPy-NSA and PPy-DBSA at different temperature ranges.

Temperature (K)	Activation energy (kcal/mol)/(10^3)			
	PPy	PPy-NSA	PPy-CSA	PPy-DBSA
300 ~ 350	1.264 ± 0.13	0.865 ± 0.15	0.0134 ± 0.05	1.466 ± 0.29
350 ~ 400	1.426 ± 0.21	1.289 ± 0.35	0.0144 ± 0.15	1.775 ± 0.25
400 ~ 450	1.711 ± 0.25	1.413 ± 0.15	0.0173 ± 0.24	2.129 ± 0.10
450 ~ 500	2.651 ± 0.14	2.450 ± 0.23	0.0185 ± 0.19	3.008 ± 0.17

Fig. 5 shows the plot of logarithm of conductivity versus inversed temperature for PPy and PPy-sulphonic acid films, which is exactly the reverse of Fig. 4. Fig. 5 shows a linear increase in the conductivity with the increase in temperature. The conductivity behavior depending on the temperature can be ascribed to the thermal energy due to the increase in temperature to excite electrons from the valence to the conduction band. Such behavior can be expressed by the Arrhenius equation.[25]

$$\sigma = \sigma_0 \exp\left(\frac{-E_a}{k_B T}\right) \quad (2)$$

where σ is the DC conductivity, σ_0 is the constant for a material, k_B is the Boltzmann constant, T is the absolute temperature, and E_a is the activation energy. Table 3 shows the values of E_a for PPy, PPy-CSA, PPy-NSA, and PPy-DBSA at different temperature ranges. If we compare the values from Table 3 it shows that E_a for PPy-DBSA is higher and PPy-CSA is smaller as compared to PPy, PPy-NSA.

In the polymer blends, the dopant ions/molecules play an important role in the transport properties. These dopant ions/molecules are usually positioned intrinsically between chains. In the conduction process interaction/morphology is a significant factor which play an important role in the charge delocalization of the polymer composite systems.[30,31] In these systems, it is very difficult to distinguish among the conduction mechanisms.[32-34] Nevertheless, experimental investigations reveal that the results can be explained effectively in terms of metallic content as well as the dominant hopping/tunneling mechanism. In such systems, the conductivity data may also be analyzed by the help of the Mott's variable range hopping model. This mechanism is frequently used for the explanation of the DC conductivity of disordered and amorphous materials for the variable-range hopping mechanism.[35] This mechanism is based on the premise that ca-

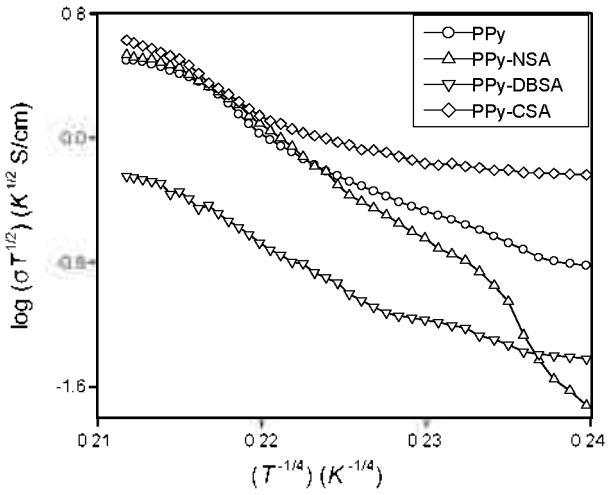

Figure 6. Plot of log ($\sigma T^{1/2}$) as a function of $T^{-1/2}$ for PPy, PPy-NSA, PPy-CSA, and PPy-DBSA.

rriers tend to hop larger distances to sites that lie energetically closer rather than to their nearest neighbors. According to this model, DC conductivity in three dimensions is derived by the following equations:

$$\sigma = \sigma_o \exp[-(T_o/T)^{1/4}] \quad (1)$$

$$\sigma_o = e^2 \nu R^2 N(E) \quad (2)$$

$$T_o = \lambda \alpha / k N(E) \quad (3)$$

where σ_o is the intrinsic conductivity at Mott's value of characteristic temperature; T_o, e is the electronic charge; ν is the hopping frequency; λ is the dimensionless constant set as 18.1 in this calculation;[36] α is the inverse rate of wave functions;[37] k is Boltzmann's constant; $N(E)$ is the density of states at the Fermi level; and

$$R = [9/8 \pi \alpha k T N(E)]^{1/4} \quad (4)$$

where R is the hopping distance. The average hopping energy W can be estimated by identifying the hopping distance R and the density of states at the Fermi level $N(E)$ by the following relation:

$$W = 3/4 \pi R^3 N(E) \quad (5)$$

By plotting log ($\sigma T^{1/2}$) versus $T^{-1/4}$, a straight line is obtained. T_o, R, $N(E)$, and W can be obtained by assuming that the conduction is three-dimensional and that it follows the variable-range model to support the analysis of our data in terms of variable-range hopping. Fig. 6 presents the log ($\sigma T^{1/2}$) versus the $T^{-1/4}$ curves for PPy, PPy-CSA, PPy-NSA, and PPy-DBSA, which shows partially straight lines and the slope (T_o) was obtained using this plot. After assuming a reasonable value of α = 10 Å and using the values of T_o, the Fermi level ($N(E)$), the average hopping energy (W), and the hopping distance (R) are determined, and they are summarized in Table 4.

Table 4. The values of T_o, R, $N(E)$, and W for PPy, PPy-CSA, PPy-NSA, and PPy-DBSA from Figure 6.

Composite	$T_o(K)$	σ_o (S/cm)	$N(E)$ (cm^{-3}) × 10^{21}	R (cm) × 10^{-7}	W (eV)
PPy	3.185×10^6	3.67	2.12	1.81	0.021
PPy-NSA	3.337×10^6	3.85	3.39	1.15	0.017
PPy-DBSA	3.192×10^6	2.94	3.43	1.22	0.021
PPy-CSA	4.866×10^6	3.98	4.54	1.72	0.032

Table 4 represents the typical values of T_o, R, $N(E)$, and W. The value of T_o implies an effective energy separation between localized states for the PPy-sulphonic acid films. The value of T_o contains geometrical parameters such as size, distance between grains, and columbic interaction energy.[38] If T_o decreases, then the system becomes highly conducting. The value of T_o for PPy-CSA is low, while it is high for PPy-DBSA, the increase in T_o in PPy-DBSA may be due to the high inter-chain distance that does not facilitate the availability of more sites for hopping in three dimensions. The values of $N(E)$, W, and R for PPy-CSA are higher compared with those of PPy-DBSA and PPy-NSA. The increase in the values of $N(E)$, W, and R suggests and supports the reason for the increase in conductivity of PPy-CSA. The overall pattern of the temperature-dependent conductivity of the PPy nanostructures is well described by Mott's law for quasi-one-dimensional variable-range hopping. The images of PPy doped with CSA shows typical granular morphology, whereas PPy doped with NSA has a cauliflower-like morphology, and PPy-DBSA has phase-segregated type morphology. It was also observed that PPy doped with NSA and DBSA is thermally stable based on the measurement of weight loss. Thus, the electrical properties of PPy can be modified by a sulfonic acid which has an influence on the morphology of the resulting PPy. The long-term stability of the electrical conductivity of PPy is a crucial property from an application point of view. Besides these, the synthesis of the nanostructure composed of PPy can enhance the electric conductivity compared with the analogue polymer bulk conductivity.

Conclusion

The PPy-CSA, PPy-NSA, and PPy-DBSA films were synthesized by *in situ* doping polymerization in the presence of CSA, NSA, and DBSA, respectively, as the dopants without an external template. The surface morphology, thermal behavior, and electrical properties of the PPy composites were modified by the use of sulphonic acid dopants. The result shows that this type of conducting polymer synthesis not only improves the poor mechanical and physical properties of heterocyclic polymers but also retains the conductivity to a desirable value. PPy films and fibers are proven to have highly sensitive electromechanical effects, allowing them to be useful as artificial valves, chemical valves, actuators, and chemomechanical materials.

Acknowledgments. This research was supported by Basic Science Research Program through the National Research Foundation of Korea (**NRF**) funded by the Ministry of Education, Science and Technology. (00042009026-00)

References

1. Vidal, J. C.; Garcia, E.; Castillo, J. R. *Anal. Chim. Acta* **1999**, *385*, 213.
2. Campbell, T. E.; Hodgson, A. J.; Wallace, G. G. *Electroanalysis* **1999**, *11*, 215.
3. Kincal, D.; Kamer, A.; Child, A. D.; Reynold, J. R. *Synth. Met.* **1998**, *92*, 53.
4. Kemp, N. T.; Flanagan, G. U.; Kaiser, A. B.; Trodahl, H. J.; Chapman, B.; artridge, A. C.; Buckley, R. G. *Synth. Met.* **1999**, *101*, 434.
5. Jerome, C.; Labaye, D.; Bodart, I.; Jerome, R. *Synth. Met.* **1999**, *101*, 3.
6. Smela, E. *J. Micromech. Microeng.* **1999**, *9*, 1.
7. Selvaraj, M.; Palraj, S.; Maruthan, K.; Rajagopal, G.; Venkatachari, G. *Synth. Met.* **2008**, *158*, 888.
8. Li, J.; Zhu, L.; Shu, B.; Tang, H. *Synth. Met.* **2008**, *158*, 516.
9. Basavaraja, C.; Choi, Y. M.; Park, H. T.; Huh, D. S.; Lee, J. W.; Revanasiddappa, M.; Raghavendra, S. C.; Khasim, S.; Vishnuvardhan, T. K. *Bull. Korean Chem. Soc.* **2007**, *28*(7), 1104.
10. Vishnuvardhan, T. K.; Kulkarni, V. R.; Basavaraja, C.; Raghavendra, S. C. *Bull. Mater. Sci.* **2006**, *29*(1), 77.
11. Iroh, J. O.; Williams, C. *Synth. Met.* **1999**, *99*, 1.
12. Cao, L.; Chen, H. Z.; Zhou, H. B.; Zhu, L.; Sun, J. Z.; Zhang, X. B.; Xu, J. M.; Wang, M. *Adv. Mater.* **2003**, *15*, 909.
13. Goren, M.; Qi, Z. G.; Lennox, R. B. *Chem. Mater.* **2000**, *12*, 1222.
14. Su, W.; Iroh, J. O. *Synth. Met.* **1998**, *95*, 159.
15. Dong, H.; Prasad, S.; Nyame, V.; Jones, W. E. *Chem. Mater.* **2004**, *16*, 371.
16. Liu, W.; Kumar, J.; Tripathy, S.; Samuelson, L. A. *Langmuir* **2002**, *18*, 9696.
17. Jang, J.; Oh, J. H.; Li, X. L. *J. Mater. Chem.* **2004**, *14*, 2872.
18. Adams, P. N.; Devasagayam, P.; Pomfret, S. L.; Abell, L.; Monkman, A. P. *J. Phys.: Condens. Matter.* **1998**, *10*, 8293.
19. Yoo, J. E.; Cross, J. L.; Bucholz, T. L.; Lee, K. S.; Espe, M. P.; Loo, Y. L. *J. Mater. Chem.* **2007**, *17*, 1268.
20. Ding, S. J.; Zhang, C. L.; Yang, M.; Qu, X. Z.; Lu, Y. F.; Yang, Z. Z. *Polymer* **2006**, *47*, 8360.
21. Zhang, F.; Halverson, P. A.; Lunt, B.; Linford, M. R. *Synth. Met.* **2006**, *156*, 932.
22. Dufour, B.; Rannou, P.; Fedorko, P.; Djurado, D.; Travers, J. P.; Pron, A. *Chem. Mater.* **2001**, *13*, 4032.
23. Dufour, B.; Rannou, P.; Djurado, D.; Janeczek, H.; Zagorska, M.; Geyer, A.; Travers, J. P. *A. Pron. Chem. Mater.* **2003**, *15*, 1587.
24. Liu, Y.; O'Keefe, M. J.; Beyaz, A.; Thomas, P. S. *Surf. Interface Anal.* **2005**, *37*, 782.
25. Yasin, S. F.; Zihlif, A. M.; Ragosta, A. *J. Mat. Sci: Materials in Electronics* **2005**, *16*, 63.
26. Lim, S. L.; Tan, K. L.; Kang, E. T. *Langmuir* **1998**, *14*, 5305.
27. Rosenberg, H. M. *Low Temperature Solid State Physics*; Oxford University Press: UK, 2000.
28. Joo, J.; Long, S. M.; Pouget, J. P.; Oh, E. J.; MacDiarmid, A. G.; Epstein, A. J. *Phys. Rev. B* **1998**, *57*, 9567.
29. Kaiser, A. K. *Rep. Prog. Phys.* **2001**, *64*, 1.
30. Hauser, J. J.; Kimerling, L. C. *Phys. Rev. B* **1975**, *11*, 4043.
31. Efros, A. L.; Shlovskii, B. I. *J. Phys. C* **1975**, *8*, 49.
32. Sheng, P. *Philos. Mag. A* **1992**, *65*, 357.
33. Zuppiroli, L.; Bussac, M. N.; Paschen, S.; Chauvet, O.; Forro, L. *Phys. Rev. B* **1994**, *50*, 5196.
34. Nair, K.; Mitra, S. S. *J. Non-Cryst. Solids.* **1977**, *24*, 1.
35. Mott, N. F.; Davis, E. A. *Electronic Processes in Non-Crystalline Materials*; Clarendon Press: Oxford, 1979.
36. Singh, R.; Tandon, R. P.; Panwar, V. S.; Chandra, S. *J. Appl. Phys.* **1991**, *69*, 2504.
37. Rouleau, J. F.; Goyette, J.; Bose, T. K. *Phys. Rev. B* **1995**, *52*, 4801.
38. Basavaraja, C.; Veeranagouda, Y.; Lee, K.; Pierson, R.; Revanasiddappa, M.; Huh, D. S. *Bull. Korean Chem. Soc.* **2008**, *29*(12), 2423.